Hydrographic and productivity characteristics along 45° E longitude in the southwestern Indian Ocean and Southern Ocean during austral summer 2004

P. Jasmine[1], K. R. Muraleedharan[1,5,*], N. V. Madhu[1], C. R. Asha Devi[1], R. Alagarsamy[2], C. T. Achuthankutty[1], Zeena Jayan[3], V. N. Sanjeevan[4], Satish Sahayak[1]

[1]National Institute of Oceanography, Regional Centre, Dr. Salim Ali Road, PB No. 1918, Kochi – 682 018, India

[2]National Institute of Oceanography, Dona-Paula, Goa – 403 004, India

[3]National Centre for Anarctic and Ocean Research, SADA, Goa, India

[4]Centre for Marine Living Resources and Ecology, Ministry of Earth Sciences, Kendriya Bhavan, PB No. 5415, Kochi, CSEZ PO, Kakkanad – 37, India

[5]*Present address:* National Institute of Oceanography, Regional Centre, Dr. Salim Ali Road, PB No. 1918, Kochi – 682 018, India

ABSTRACT: During the austral summer 2004, an intensive multidisciplinary survey was carried out in the Indian Ocean sector of the Southern Ocean to study the main hydrographic features and the associated productivity processes. This sector includes circumpolar zones and fronts with distinct hydrographic and trophic regimes, such as the Subtropical Zone (STZ), Subtropical Frontal Zone (STFZ), Subantarctic Zone (SAZ), Polar Frontal Zone (PFZ), North Subtropical Front (NSTF), Agulhas Retroflection Front (ARF), South Subtropical Front (SSTF), Subantarctic Front, Surface Polar Front (SPF), and Subsurface Polar Front. Seasonal variations in the solar irradiance and day length, stratification, lack of micronutrients like iron and increased grazing pressure are the major factors that influenced or constrained biological production in this region. Even though broad differences in these controlling factors exist in time and space between the zonal regions, the upper 1000 m of the water column of the main zones, STZ, STFZ, SAZ, PFZ, supported almost identical standing stocks of mesozooplankton, 0.43, 0.47, 0.45 and 0.49 ml m^{-3}, respectively, during the austral summer. This unexpected similarity can be explained either through the functioning of the microbial loop within STZ, STFZ and SAZ and the multivorous food web ecology within the PFZ. Dominance of ciliates in the microzooplankton community may be one factor resulting in the maintenance of a high mesozooplankton standing stock in SAZ. In contrast to the zones, frontal regions showed wide differences in hydrography and biological characteristics. The SSTF and SPF were far more biologically productive than that of NSTF and ARF.

KEY WORDS: Fronts · Zones · Microzooplankton · Mesozooplankton · Microbial loop · Southern Ocean

INTRODUCTION

The Southern Ocean plays a major role in regulating the global carbon fluxes and the world's climate. Tropical regions are characterised by receiving a surplus of solar energy whereas the polar regions are in deficit of this energy not only during winter with either long or continuous nights, but also during summer because of the sun's low angle of incidence. Both atmospheric and oceanic circulations regulate the global carbon budget by exporting the surplus energy from tropical to polar regions. Fronts and the water masses of the Southern Ocean greatly influence the regulation of biological production at the global scale (Abrams 1985). Huntley

et al. (1991) reported that seabirds and mammals may transfer 20 to 25% of photosynthetically fixed carbon into the atmosphere via respiration after consuming macrozooplankton and micronekton. Therefore, zooplankton occupies an important position in the Southern Ocean carbon cycle.

The major current system in the Indian Ocean sector of the Southern Ocean is the Antarctic Circumpolar Current (ACC). The principal mechanism determining the different properties within the zones and along the frontal systems is the wind-induced transport (from the westerlies) that drives the uninterrupted eastward flowing ACC. Deacon (1933, 1937) was the first to outline the frontal systems in the Southern Ocean and suggested that they are circumpolar and other studies followed (Lutjeharms 1981, Deacon 1982, 1983, Belkin & Gordon 1996, Holliday & Read 1998, Froneman et al. 2000, Pollard & Read 2001). Along the 45° E longitude the main features are (from north to south), the existence of the North Subtropical Front (NSTF), Agulhas Retroflection Front (ARF), South Subtropical Front (SSTF), Subantarctic Front (SAF) and Polar Front (PF); the PF has both Surface Polar Front (SPF) and Subsurface Polar Front (SSPF) expressions. These frontal systems subdivide the sector into zones with different biogeochemical characteristics, viz. the Subtropical Zone (STZ), Subtropical Frontal Zone (STFZ), Subantarctic Zone (SAZ) and Polar Frontal Zone (PFZ) with the Surface Polar Zone (SPZ) and the Subsurface Polar Zone (SSPZ) at 200 m. The Antarctic Paradox is related to a well-known phenomenon referred to as the high nutrient low chlorophyll (HNLC) condition, i.e. there are regions where N and P are in high concentrations throughout the year, but primary productivity is low. The SAZ and the SAF exhibit the HNLC phenomenon prominently in the Southern Ocean (El-Sayed 1984). Four major hypotheses are put forward to explain the paradox: (1) insufficient solar energy for phytoplankton growth to attain its full potential (Nelson & Smith 1991), (2) deficiency of micronutrients like iron (Martin et al. 1990a,b), (3) strong winds that stir the water and result in deepening of the mixed layer and convection (Sakshaug et al. 1991), and (4) grazing by zooplankton (Dubischar & Bathmann 1997).

The major currents that make this region so dynamic are the Agulhas Current and the ACC. The Agulhas Current (Gordon 1985) is the western boundary current that flows poleward along the east coast of Africa from 27° to ca. 40° S, and then reverses direction or retroflects eastwards to become the Agulhas Retroflection Current. The retroflection exhibits a quasi-stationary meandering pattern with a wavelength of 500 km between 38° and 40° S (Gordon 1985). The westerlies are largely confined between ca. 40° and ca. 65° S and drive the eastward surface current,

initiating a northward Ekman drift that is critical to the formation of the Antarctic Intermediate Water mass (AIW), subducted below the subantarctic surface water. The strong circumpolar geostrophic currents and weak stratification result in the isopycnals tilting towards the surface in the southern part of ACC. This tilting brings in deep water upwelling originating from the other oceans and also from the deep Indian Ocean to the surface where they are modified by atmospheric interactions. Another feature that results in the upwelling of nutrient-rich deep water to the surface is the Antarctic Divergence (Jones et al. 1990). The upwelling deep water contains not only high concentrations of dissolved nutrients that support rich biological productivity, but is also supersaturated with CO_2 that is vented to the atmosphere and plays a substantial role in modulating atmospheric CO_2 concentrations. The biological pump is another mechanism whereby atmospheric CO_2 concentrations can be drawn down and transferred into the deep ocean. CO_2 converted into organic matter by photosynthesis is exported to deeper waters from the upper ocean by sedimentation and vertical migrations of organisms. The westerlies have a large effect on the Southern Ocean hydrography, exerting a great influence on both the distribution of sea ice and biological productivity. However, in oceanic waters beyond the influence of land masses, phytoplankton production of this region is consistently lower than would normally be expected in Southern Ocean waters with high macronutrient concentrations (Boyd et al. 2000).

The degree of variability in hydrographic and biological characteristics is high between the zones and frontal system (Kostianoy et al. 2003, 2004). Macroscale zonation of the epipelagic zooplankton in the Southern Ocean has been extensively investigated (e.g. Grachev 1991, Pakhomov & McQuaid 1996, Froneman et al. 2000). Although many studies have been conducted in the Pacific and Atlantic ocean sectors, the Indian Ocean sector still remains mostly unexplored. A few studies in the Indian Ocean sector have focused in the vicinity of a major front or zone (Bernard & Froneman 2003, 2005, Froneman et al. 2007) and the waters surrounding the oceanic islands (Fielding et al. 2007). However, an extensive study of the response of biological communities from the subtropical to polar regions is still lacking. In addition, whether HNLC affects the secondary productivity in the different zones has also not yet been fully understood. The 2 major objectives of this study were to describe the response of biological communities to different fronts and zones by switching to a food web structure better adapted to the varying environment, and to understand the influence of HNLC on the secondary trophic level.

MATERIALS AND METHODS

Hydrographic and biological measurements in the Indian Ocean sector of the Southern Ocean were carried out onboard the FORV 'Sagar Kanya' during the austral summer (January to February 2004). Observations were made along the 45° E longitude, from 30° S to 55° S (Fig. 1), which passes through the major fronts and zones between the subtropical and polar regions. Hydrographic observations were taken at 1° latitudinal intervals, while the biological samples were collected at 2° intervals. A SBE Seabird 911 plus CTD was used for recording temperature (accuracy ± 0.001°C) and salinity (conductivity ± 0.0001 S/m) profiles up to 1000 m depth with a bin size of 1 m. Salinity values from the CTD were calibrated against the values obtained from water samples measured using the Autosal (Guildline 8400A) onboard. The sea surface temperature (SST) was measured using a bucket thermometer (accuracy ± 0.2°C). Advanced very high resolution radiometer (AVHRR) SST (spatial resolution 4 km and temperature accuracy of about ± 0.3°C) were recorded over the time span of the cruise and averaged for analysis. Surface meteorological parameters (air temperature, wind speed and direction) were recorded at all stations. Plots of potential temperature versus salinity identified the water masses and frontal structures. QuikSCAT satellite data were used to study the prevailing wind patterns. Data from altimetric sensors mounted on the satellites (TOPEX/POSIDON, JASON-1 and GFO) of NOAA were collected, processed and averaged during the cruise period.

Water samples were collected with a rosette sampler from standard depths (0, 10, 20, 30, 50, 75, 100, 150, 200, 300, 500, 750 and 1000 m) and analyzed for nitrate, phosphate and silicate with a segmented flow autoanalyzer (model 51001-1, Skalar Analytical BV) (Grasshoff et al. 1983). Dissolved oxygen (DO) was estimated by the Winkler method (Carpenter 1965) as follows. Water samples from the standard depths were carefully collected without trapping air bubbles in 125 ml glass bottles and immediately fixed by adding 0.5 ml of Winkler A solution (manganese chloride) and 0.5 ml of Winkler B solution (alkaline potassium iodide). Samples were then mixed well and allowed to precipitate. After acidification with 50% HCl, the samples were titrated against a standard sodium thiosulphate solution using starch as an end-point indicator. The titration was based on iodimetry with a Dosimat and the end point determined visually when the blue colour disappeared.

CTD data were used to locate the maximum surface gradients in temperature and salinity fields to understand the water masses and frontal systems structures. Sharp gradients in temperature and salinity were observed across the frontal systems; otherwise the temperature and salinity (i.e. water mass structure) remained more or less constant across the hydrographic zones between the fronts.

Validation and estimation of the remotely sensed chlorophyll *a* and modeling of primary production with *in situ* observation. For *in situ* chlorophyll *a* (chl *a*) and primary productivity measurements, water samples were collected from 7 discrete depths according to the Joint Global Ocean Flux Study (JGOFS) protocols (UNESCO 1994). For chl *a* measurements, 2 l of water from each depth were filtered through GF/F filters (pore size
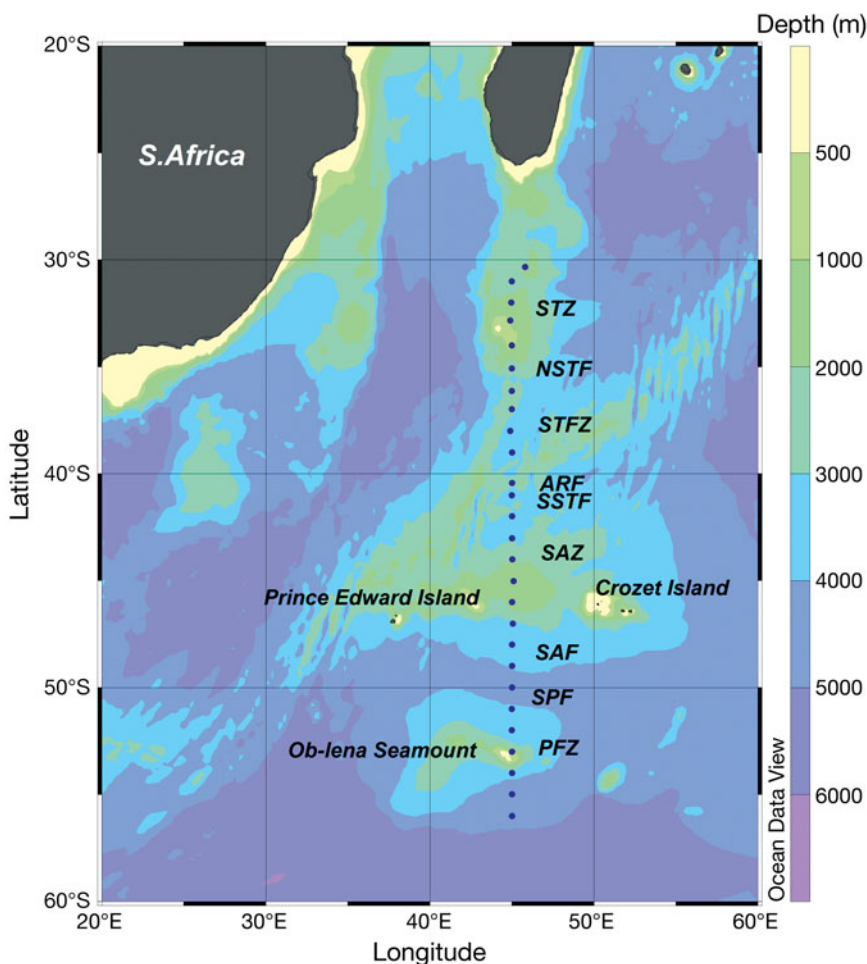

Fig. 1. Study area showing station positions overlaid on a bathymetric chart that includes nearby islands and seamounts of the area sampled for hydrographic (1° S) and biological studies (2° S) during January to February 2004

0.7 µm), extracted with 10 ml of 90% acetone and analyzed with a UV/Vis spectrophotometer (Perkin–Elmer). Water samples for measurement of primary productivity were collected before sunrise and incubated *in situ* for 12 h after adding 1 ml of Na[^{14}H]CO$_3$ to each sample (5 µCi per 300 ml seawater). After incubation, the samples were filtered through 47 mm GF/F (pore size 0.7 µm) filters under gentle suction, exposed to concentrated HCl fumes to remove excess inorganic carbon and kept in scintillation vials. Scintillation cocktail was added to the vials 1 d before the analysis, and the activity was counted in a scintillation counter (Wallace). The disintegrations per minute (dpm) values were converted into daily production rates (mg C m^{-3} d^{-1}) using the formula of Strickland & Parsons (1972). Column chl *a* (mg m^{-2}) and column primary production (mg C m^{-2} d^{-1}) were estimated by integrating the depth values.

To understand the primary production and associated biological process that happens in the merged frontal regions and small scale processes, the study required fine resolution data sets. Such a high resolution *in situ* measurement is not possible because of time constraints during the cruise. The *in situ* chl *a* and primary productivity measurements were done at 2° latitudinal intervals only. Fortunately, remote sensing technique can yield high resolution but less accurate data than *in situ* techniques on both spatial and temporal scales. But careful analysis and application of the correction for sea surface and atmospheric conditions by incorporating real-time meteorological data will yield highly accurate data. SeaDAS software was used to process the remotely sensed geophysical data with an algorithm for sea surface and atmospheric correction to generate high accuracy output. MODIS-Aqua SST data during the night pass was processed to a 9 km spatial and 8 d temporal resolution during the cruise period and were used for the present study. The Seaviewing Wide Field-of-view Sensor (SeaWiFS) is an 8-channel visible light radiometer dedicated to global ocean color measurements that are used to detect and analyze patterns of biological activity in the marine environment. SeaWiFS covers more than 90% of the ocean surface every 2 d. The output data binned to a spatial resolution of 9 km and temporal resolution of 8 d were used for the present study. We used chl *a* concentration and photosynthetically available radiation data from the SeaWiFS and the SST data from the aqua-MODIS satellite for the duration of the cruise to derive phytoplankton concentrations and oceanic primary productivity.

SeaWiFS measures the total amount of chlorophyll concentration in the euphotic zone (Z_{eu}). Physical depth of the euphotic zone is defined as the penetration depth of 1% surface irradiance based on the Beer-Lambert's law (Morel & Berthon 1989). Z_{eu} is calculated from chlorophyll (C_{sat}) following Morel & Berthon (1989). For the comparison and validation of remotely sensed chlorophyll to *in situ*, we have done the integration of *in situ* chlorophyll from surface to Z_{eu} by trapezoidal integration.

Behrenfield & Falkowski (1997a) developed a vertically generalized production model (VGPM) that relates the chlorophyll concentrations to depth integrated Z_{eu} primary production (PP), as follows:

$$\sum PP = 0.66125 \times \left[\frac{E0}{E0 + 4.1} \right] \times P^b_{opt} \times C_{sat} \times Z_{eu} \times D_{irr} (mgCm^{-2}d^{-1})$$

The core of the VGPM, like other depth-integrated models, which include a measure of depth-integrated phytoplankton biomass, estimates the C_{sat} and Z_{eu}, as well as inclusion of an irradiance-dependent function ($E0$) and a photo-adaptive yield term P^b_{opt} necessary to convert the estimated biomass into a photosynthetic rate (Behrenfield & Falkowski 1997b). The factor P^b_{opt}, which is the optimal environment for the maximum carbon fixation rate, measured as mg C (mg chl)$^{-1}$ h^{-1}, within the water column, is the only model parameter that is neither relatable to the chlorophyll, nor possible to measure remotely. We adopted Behrenfield & Falkowski (1997b) for the computation of the factor, which relates the optimal environment to the SST for the maximum primary production. According to the geographical position and time of year, the amount of the incoming solar irradiance varies, which can be computed from Bird's (1984) clear sky spectral irradiance model, with modifications suggested by Sathyendranath & Platt (1988). Day length (D_{irr}) is also included in this model, to scale observational data from hourly incubations to daily rates.

Sampling of both micro- and mesozooplankton was carried out at alternate stations. Microzooplankton was sampled by collecting 10 l of water at standard depths (surface, 10, 20, 50, 75, 100 and 120 m). The water samples were initially screened through a 200 µm mesh bolting-cloth net to remove mesozooplankton, and then filtered through 20 µm mesh bolting silk to retain the microzooplankton. Each microzooplankton sample was then backwashed gently with filtered seawater (20 µm mesh size); volumes were made up to 500 ml and preserved by adding 1% acid Lugol's iodine. All samples were further concentrated by siphoning out the excess water through a 20 µm filter and left to settle for >48 h. Microzooplankters were enumerated and identified (Olympus inverted microscope, (100 and 400×). Ciliates and dinoflagellates, larval stages of metazoans, radiolarians and foraminiferans were identified to group level.

Mesozooplankton samples were collected with a multiple plankton net (MPN, Hydrobios) (mouth area 0.25 m², mesh size 200 μm). Vertical hauls divided the upper 1000 m into 4 depth strata: (1) 1000 to 500 m, (2) 500 to bottom of thermocline (BT), (3) BT to top of thermocline (TT), (4) TT to surface. Samples were fixed in 5% formaldehyde. Biomass was determined by volume displacement and expressed as ml m⁻³ of water filtered. Major zooplankton taxa were sorted from 25% aliquots. Abundance of individual taxa (individuals [ind.] m⁻³) was calculated for the whole sample and converted to percentage composition. Recent studies (Nielsen et al. 2004, Jaspers et al. 2009) suggest that small fractions of zooplankters may be drained off and lost when a 200 μm mesh net is used for samples from oligotrophic waters. Thus, in this study at each station both microzooplankton (20 to 200 μm) and mesozooplankton (>200 μm) were collected and analysed to avoid the underestimation of numbers of small sized zooplankters.

RESULTS

The maximum SST (Fig. 2) of 25.3°C was observed at STZ where the surface salinity was about 35.6, while the minimum of 2°C was recorded at PFZ. The position of the ARF observed was in agreement with that of Lutjeharms & Valentine (1984). SST decreased in ARF by 1.9°C (Fig. 2) from the STFZ value of 18.6°C and the average sea surface salinity (SSS) was 35.6. Across the SSTF, a sharp decrease in SST (18.57 to 13.1°C) and SSS (35.61 to 34.16) were noticed. The vertical section of temperature and salinity (Fig. 3a,b) showed that the expression of this front extended down to 900 m. SAZ is a region where temperature stratification was more intense compared with the salinity stratification. Compared with other regions, the salinity minimum zone was noticed in the SAZ and was associated with AAIW. This zone is the limit of the warm and saltier waters, typical of the subtropical regions with a thermostad (Fig. 3a) between 200 and 400 m. The temperature and salinity section (Fig. 3a,b) in the SAF showed a weak gradient at the surface between 47°S and 48°S, denoting the frontal boundary between subantarctic surface water (SASW) and polar surface waters. The mean position of the SPF, according to surface and subsurface expressions, was at ca. 50°S, where SST (Fig. 2)

was 3.8°C and SSS was 33.79. We observed the subsurface polar front between 51°S and 55°S with the 2.0°C isotherm clearly demarcating the surface and subsurface expressions of the polar front. The sections of the temperature and salinity (Fig. 3a,b) showed the northward extension of the low temperature (<2.0°C) and fresher water mass at depths of 100 to 400 m, where salinity remained relatively constant at 34.2 to 34.6.

Strong, zonally prevailing, westerly winds forced large, near-surface, northward Ekman transport creating a northward pressure gradient. The ACC is approximately in geostrophic equilibrium, with isopycnals inclined towards the surface layer of the polar region. Geostrophic currents (from thermohaline profiles) also showed a strong band of an eastward flowing current (40 cm s⁻¹) between 41°S and 43°S with a vertical extension of 800 m (Fig. 4b).

Surface DO values were relatively low (ca. 225 μmol) between 30°S and 35°S and increased to 310 μM between 39°S and 43°S (Fig. 5a). Farther south, DO gradually increased to reach a maximum of 360 μM at
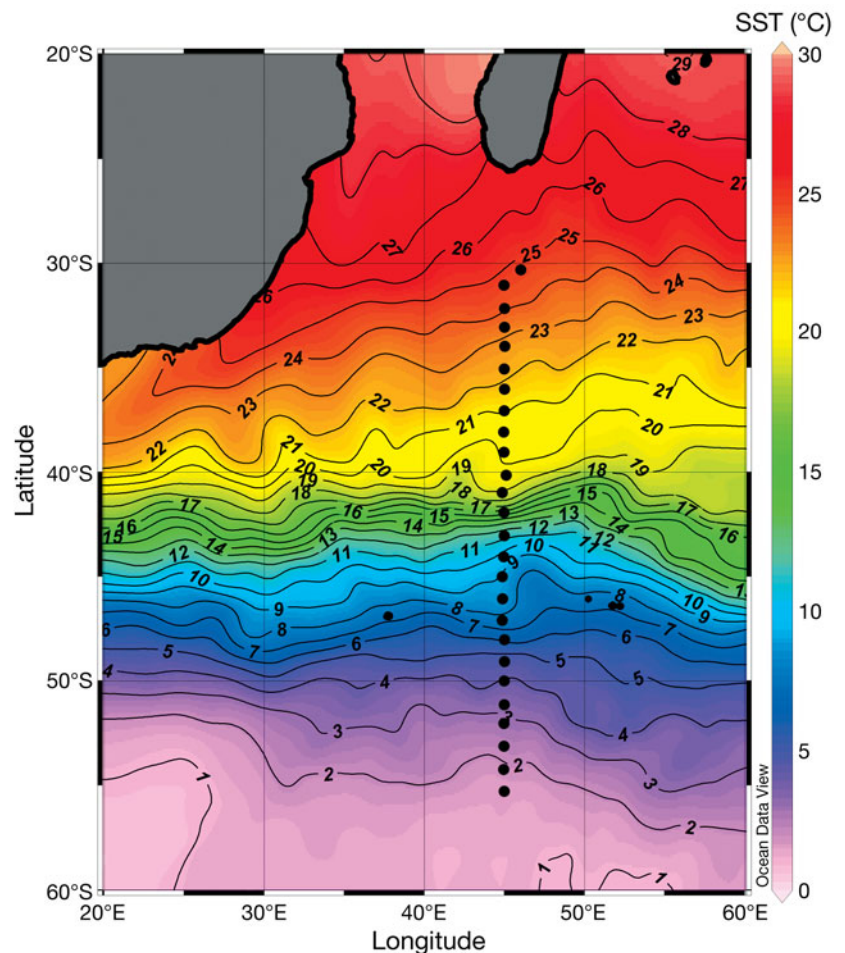

Fig. 2. Sea surface temperature (SST) data from MODIS-aqua is posted with station positions showing strong gradients of temperature in the fronts and lesser gradients of temperature in the zones
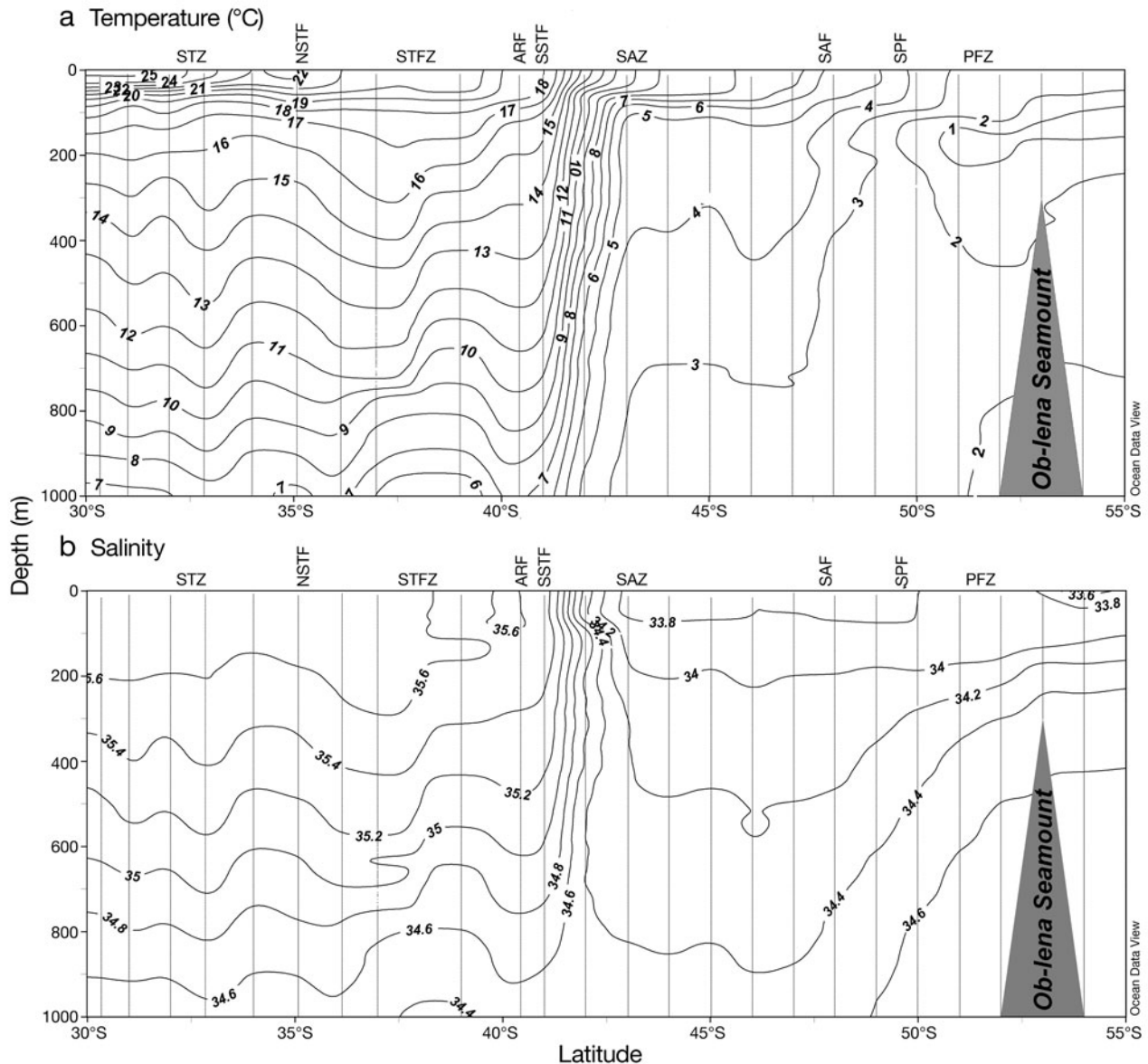
Fig. 3. Vertical section of (a) temperature (°C) and (b) salinity. The frontal feature can be observed where the temperature and salinity exhibit steep meridional gradients (i.e. where the contours are closest together) and fewer contours in the zonal regions. STZ: Subtropical Zone; NSTF: North Subtropical Front; STFZ: Subtropical Frontal Zone; ARF: Agulhas Retroflection Front; SSTF: South Subtropical Front; SAZ: Subantarctic Zone; SAF: Subantarctic Front; SPF: Surface Polar Front; PFZ: Polar Frontal Zone

54°S (Fig. 5a). Surface DO was found to be inversely correlated (r^2 = 0.96) with SST (Fig. 6a), and positively correlated (r^2 = 0.324) with wind speed (Fig. 6b). Surface macronutrients (Fig. 5b–d) were consistently low between 30°S and 40°S (nitrate ca. 1 µmol, phosphate ca. 0.18 µmol and silicate 6 µmol). However, south of 41°S, nitrate concentrations (Fig. 5b) rose sharply to attain a maximum of 27.5 µmol at 51°S, but declined to 10 µmol at 55°S. Surface phosphate concentrations (Fig. 5c) rose south of 43°S to a maximum of 1 µmol, which was sustained between 49°S and 53°S, but declined to 0.17 µmol at 55°S.

During the austral summer, the maximum intensity of solar radiation (Fig. 7a) was calculated to be 475 to 400 W m^{-2} between 30°S to 55°S and the day length (Fig. 7b) increased southwards from about 14 to 18 h. The photosynthetically available radiation (PAR) estimated from SeaWiFS showed a zonal pattern, with high radiation (>50 E m^{-2} d^{-1}) at 30°S that declined to <30 E m^{-2} d^{-1} at 55°S. The calculated euphotic zone had a potential depth range of 50 to 70 m between 40°S and 50°S, and increased to 70 to 90 m towards the equator. During this period, the average surface chl a concentration (Fig. 8a) was high (1.0 mg m^{-3})
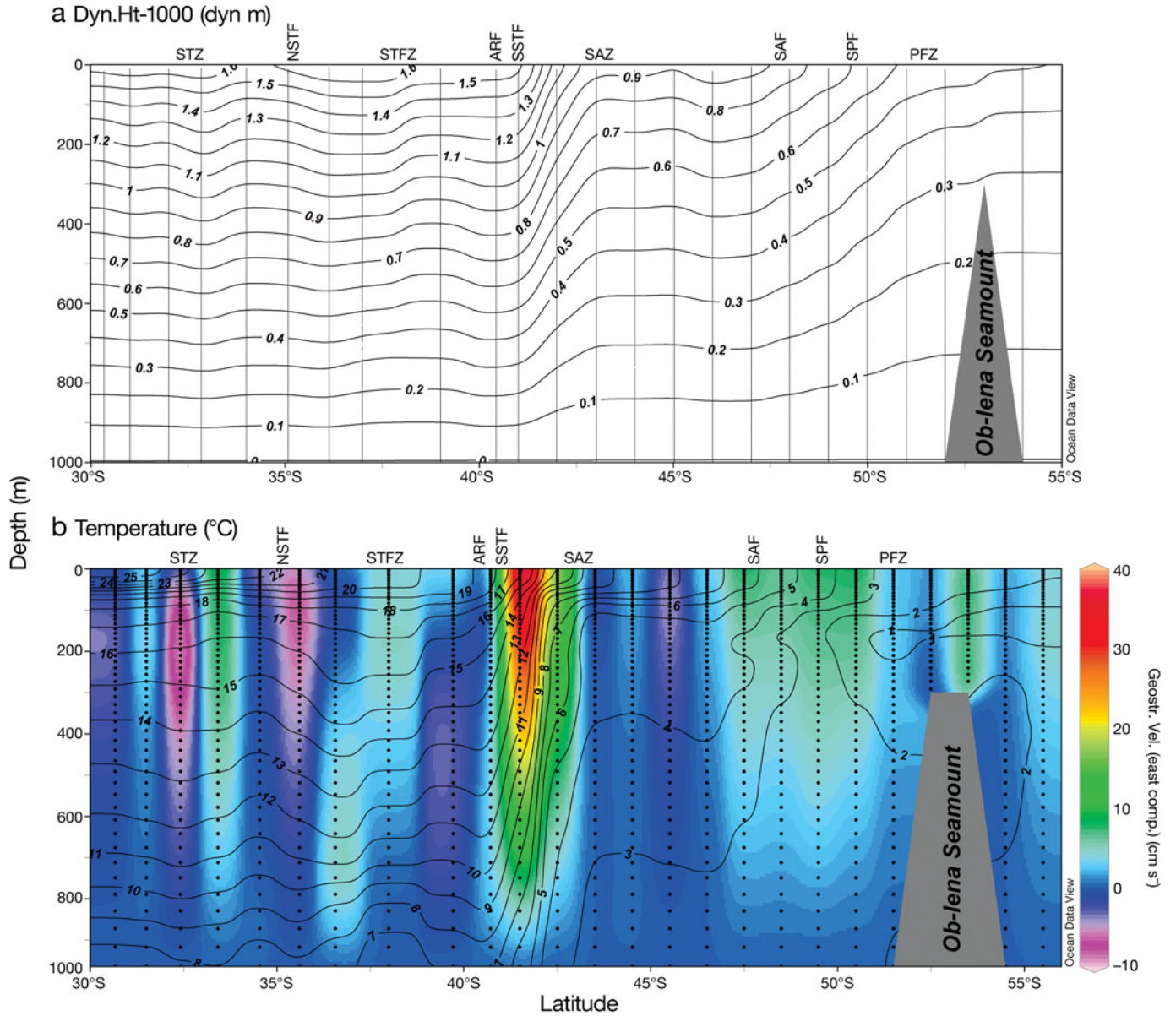
Fig. 4. Vertical section of (a) dynamic height with respect to 1000 m (b) geostrophic current (coloured) overlaid with temperature (°C) contours showing strong flow patterns in the fronts and weak flow patterns in the zonal regions. Strong geostrophic currents coincided with the temperature gradients at ARF and SSTF. See Fig. 3 for abbreviations

between 41° S and 43° S, but was low (0.08 mg m⁻³) in other areas, except at the PF where it reached 0.2 mg m⁻³.

The linear relation between *in situ* and remotely sensed chl *a* had a correlation (r^2) of 0.43 and yielded a validation relation for remotely sensed chl *a* as:

Corrected remotely sensed chlorophyll = 1.83 × *in situ* chl *a* + 0.03

This correction was applied to SeaWiFS chlorophyll (Fig. 8b) that showed high chl *a* concentrations of >7 mg m⁻³ between 41° S and 42° S. The linear relationship between *in situ* PP and that estimated

from the vertically generalized production model (VGPM) showed a correlation (r^2) of 0.41 and yielded a validation relation for modelled primary production as:

Corrected primary production (VGPM) = 22.62 × *in situ* PP + 98.23

Results showed a zone of high column productivity of 400 to 1000 mg C m⁻² d⁻¹ between 39° S and 43° S with a maximum of 1000 mg C m⁻² d⁻¹ at 42° S (Fig. 9). Primary production rates decreased both northwards to 20° S (to 200 mg C m⁻² d⁻¹) and southwards to 55° S (to 100 mg C m⁻² d⁻¹).
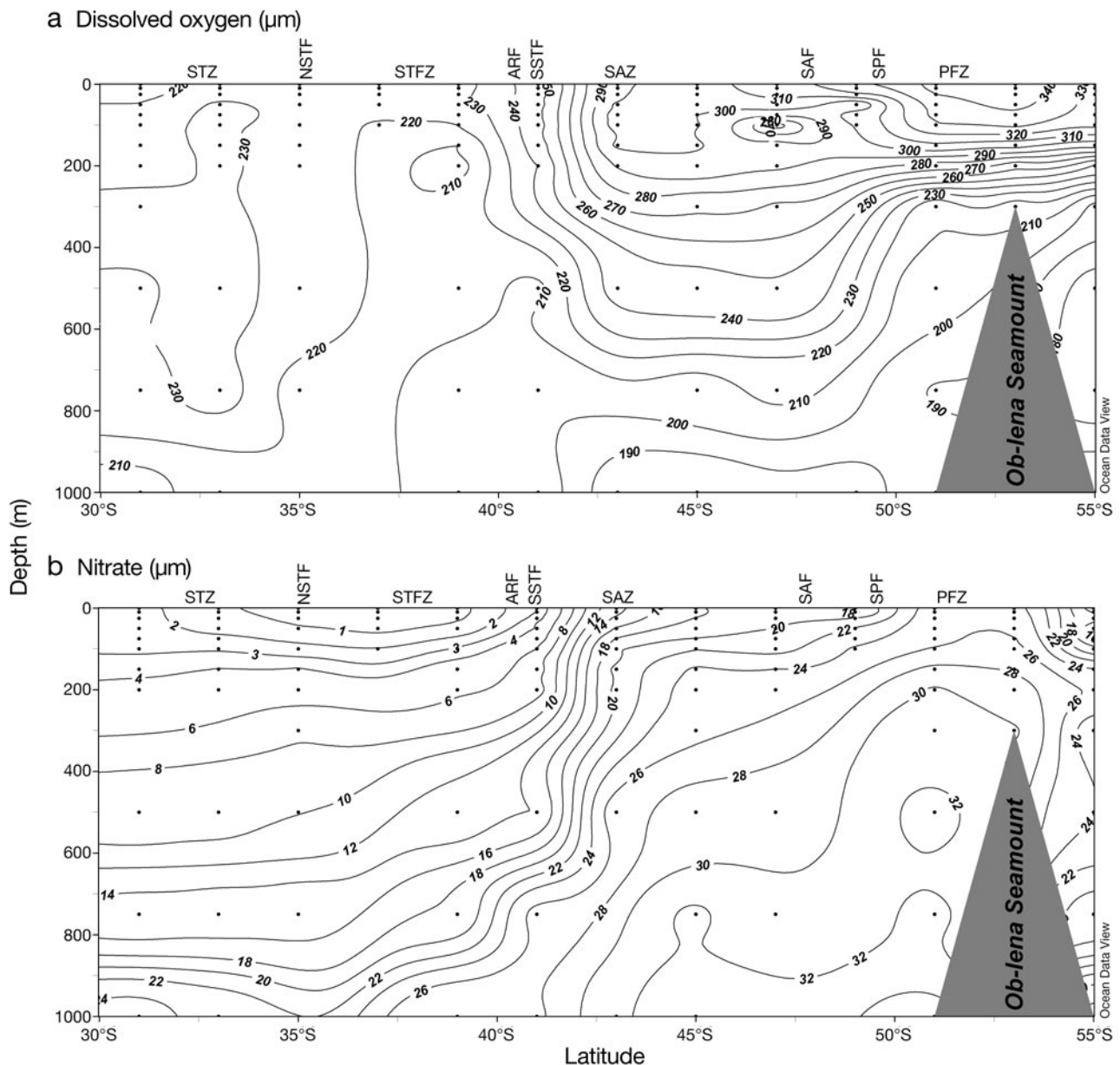
Fig. 5. Vertical section of (a) dissolved oxygen, (b) nitrate, (c) phosphate and (d) silicate concentration (µmol) contours up to 1000 m showing sharp gradients in their properties in the fronts and uniform concentrations in the zonal regions along the 45° E meridian. High concentrations of dissolved oxygen and nutrients were seen south of the SSF. See Fig. 3 for abbreviations

The microzooplankton density in the surface layer increased in the vicinity of the SPF (139×10^3 ind. m^{-3}) and SAF (80×10^3 ind. m^{-3}), and decreased at the PFZ (2.80×10^3 ind. m^{-3}). Frontal regions north of the subtropical convergence (30° S to 42° 30′ S) possessed fewer microzooplankton than those in the south. Fronts sustained relatively high microzooplankton abundance than did the zones except at SAZ where the density was 79.4×10^3 ind. m^{-3}. The upper 120 m also showed similar trend as that of the surface layer. Each zone and front was identified and characterised by a unique composition of micro-

zooplankton community (Fig. 10a,b). At SPF the microzooplankton community was dominated by ciliates (53 %), dinoflagellates (16 %) and nauplii (26.5 %), but at SAF, the composition changed and the contribution of ciliates fell to 19 %, and that of dinoflagellates and nauplii increased to 36.5 and 25 %, respectively. North of SSTF, the contribution of ciliates (>50 %) to the microzooplankton community was higher than south of SSTF, except at SAZ (84 %). The maximum contribution of ciliates (84 %) to the microzooplankton community coincided with that of SAZ.
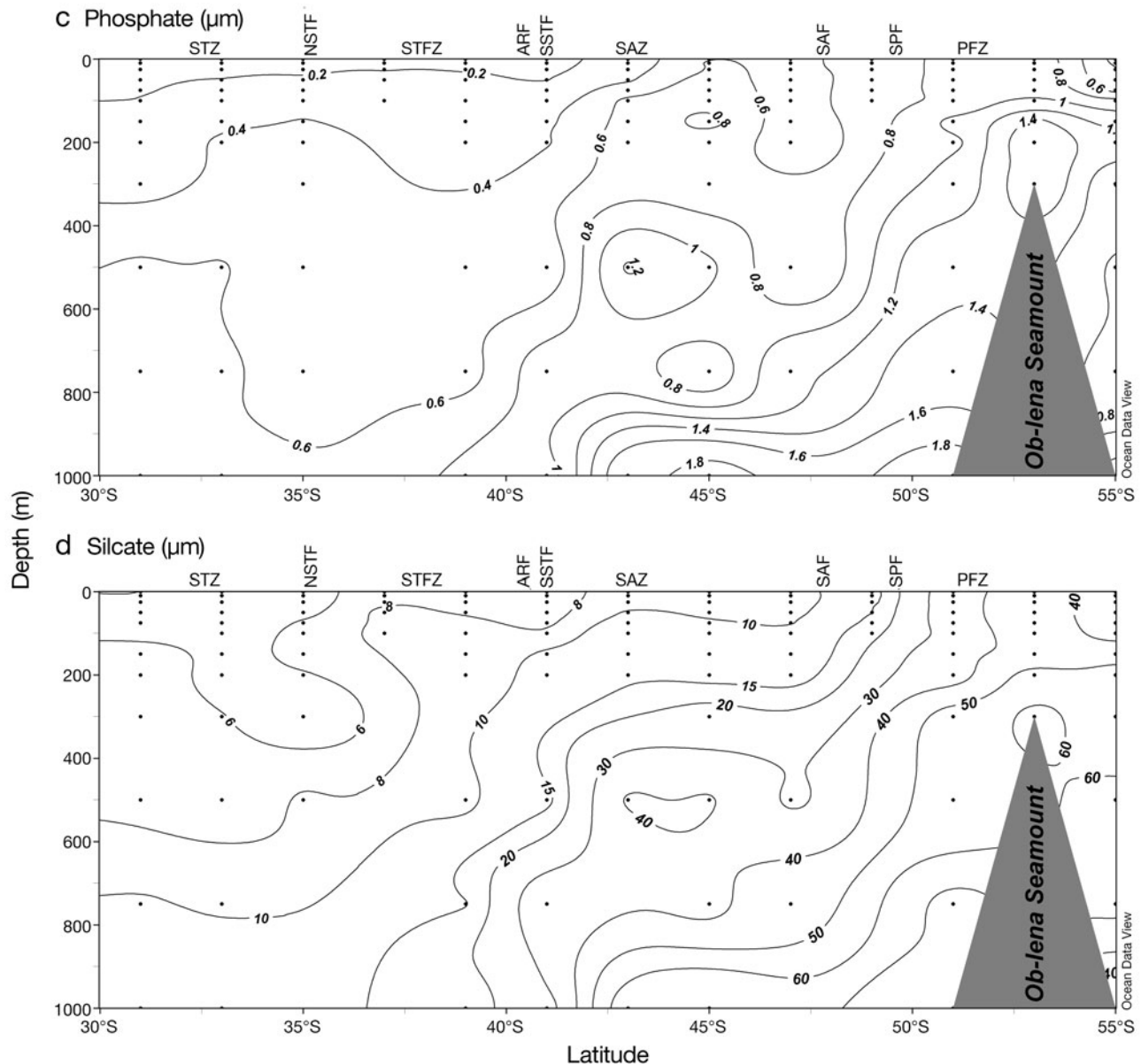
Fig. 5. Continued

Between 30° S and 55° S, high zooplankton biomass in the mixed layer was recorded at PFZ (50° S to 55° S). Among the fronts, mesozooplankton biomass was high in the mixed layer of SSTF, between 41° 15′ S and 42° 30′ S. However, compared with all other zones and frontal regions, mesozooplankton biomass (Fig. 11a,b, Table 2) was extremely low (0.010 ml m⁻³) in the mixed layer and in the upper 1000 m (0.018 ml m⁻³) of the ARF (Fig. 11a). The major components of the mesozooplankton community (Fig. 11b) in ARF were copepods (53.57%), chaetognaths (42.86%) and ostracods (3.57%). An interesting feature observed was that in the upper 1000 m; the mesozooplankton standing stock remained consistent between different zones (STZ,

STFZ, SAZ and PFZ), despite the variations in hydrographic conditions and mesozooplankton composition across the fronts (Table 2). The regions SSTF (41°15′ S to 42° 30′ S) and SAZ (43° S to 47° S) were characterised by a high incidence of euphausiids (68 and 49%, respectively), while in the other regions copepods formed the bulk of the community (>90%).

DISCUSSION

In the STZ, surface waters are warm (Figs. 2 & 3a), high in salinity (Fig. 3b) and nutrient-poor (Fig. 5b–d). The subduction of these nutrient-poor surface waters
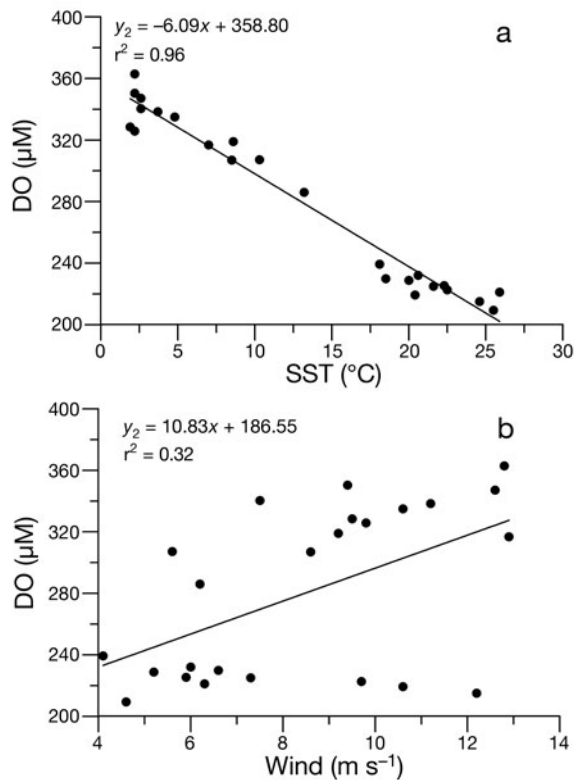
Fig. 6. Correlation of dissolved oxygen (DO) with (a) sea surface temperature (SST) and (b) wind speed showing that SST has greater influence on DO concentration than wind mixing
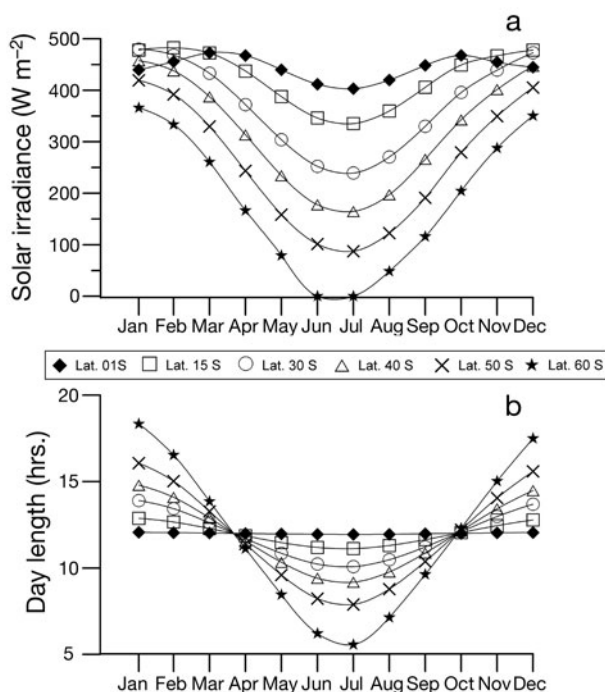

Fig. 7. Seasonal patterns of (a) solar irradiance and (b) day length showing that during the study period (austral summer), light is not a constraint for the biological production in the study area

as a result of the anticlockwise subtropical gyral circulation leads to highly oligotrophic conditions (Karstensen & Quadfasel 2002). The low chl *a* (<0.1 mg m^{-3}) and low primary production (<250 mg C m^{-2}) in this region clearly indicate oligotrophic water (Figs. 8 & 9). This is maintained almost throughout the yr except during July to September (Fig. 8b). The seasonal variations in the solar irradiance (Fig. 7a,b) of 200 to 450 W m^{-2} and the day length of 9 to 15 h indicate that the low primary production was not due to light limitation. The most likely causes for the low primary production in the region may be the combined effect of the low nutrient concentrations in the euphotic zone and the thermocline depth exceeding the compensation depth and high stability due to stratification. Surprisingly, we observed high mesozooplankton standing stock (0.440 ml m^{-3}) in the upper 1000 m (Fig. 11a,b) in this region despite the prevailing oligotrophy and low primary production. Incidentally, the biomass value showed close similarity with those of STZ (0.41 ml m^{-3}), STFZ (0.470 ml m^{-3}), SAZ (0.445 ml m^{-3}) and PFZ (0.50 ml m^{-3}). Microbial food web is known to support high mesozooplankton production in the low-nutrient low-chlorophyll systems (Azam et al. 1983, 1991, Hall et al. 1999), thereby replacing the primary producers (phytoplankton) as the source of nutrition. The occurrence of a relatively high microzooplankton community (Fig. 10a,b), dominated by ciliates (2203 × 10^3 ind. m^{-3}, 65%), indicates the possibility of strong microbial food web operating in this region. We observed maximum density of ciliates (2819 × 10^3 ind. m^{-3}) in STZ, which was in contrast with the minimum density of ciliates (108 × 10^3 ind. m^{-3}) in the PFZ. Bradford-Grieve et al. (1997) reported that significant proportions of the phytoplankton stock were in the size range of picoplankton, and ciliates were the dominant grazers of both the pico- and nanoplankton. Low phytoplankton density with high abundance of picoplankton has been reported from the subtropical north Pacific Ocean (Odate 1994). The flow cytometry data (Detmer & Bathmann 1997) also showed that autotrophic pico- and nanoplankton may contribute up to 90% of total chl *a* present in other oligotrophic regions. Under high nitrate conditions, large size classes of phytoplankton usually flourish, whereas in nitrate-depleted waters, picoplankton predominate (Taguchi et al. 1992, Calbet et al. 2001) and these populations can support a substantial amount of secondary (zooplankton) production through the microbial food web. Thus, the low availability of the large sized phytoplankton initiated the need for alternating food sources for the mesozooplankton. The trophic role of microzooplankton in supporting the high abundance of mesozooplankton is evident from the high abundance of ciliates. The relatively high biomass of micro-

Fig. 8. (a) SeaWiFS chl *a* (mg m^{-3}) concentration overlaid with advanced very high resolution radiometer sea surface tempera-tures contours during the study period. Maximum chl *a* concentration was seen in the South Subtropical Front (SSTF) and mini-mum was at the Subtropical Zone. (b) Monthly distribution of SeaWiFS chl *a* along 45° E from June 2003 to June 2004 showed highest chl *a* concentration was during November to February

zooplankton indicates a strong coupling between the mesozooplankton and the microbial food web. Satapoomin et al. (2004) also reported that microzooplankton is the major feed of mesozooplankton in oligotrophic waters.

We observed the NSTF (Belkin & Gordon 1996) between 34° S and 35° S in the southern Indian Ocean where it formed the boundary for warm, saline subtropical water and was well expressed in subsurface features (Figs. 2 & 3a,b). Primary productivity and zooplankton biomass and abundance decreased sharply across the front (Figs. 8a & 11a,b). Compared with other frontal features, the biological production associated with this front was low. The higher abundance of microzooplankton (Fig. 10a,b) in the NSTF (3046 × 10^3 ind. m^{-2}) clearly indicates the extreme oligotrophic nature of this front.

The STFZ (Lutjeharms et al. 1993) region is bounded by the NSTF to the north and the ARF to the south. In this region biological production was low as in the subtropical region despite receiving ample solar irradiance and day length of sufficient duration. But, seasonal chl *a* con-

centrations show that it is a low productivity region throughout the year. However, the relatively high abundance of the microzooplankton (Fig. 10a,b) (2819 × 10^3 ind. m^{-2}) might be sufficient enough to sustain a fairly high mesozooplankton biomass, and it was similar to the biomass values observed in the other zones. Earlier studies have indicated that the low productivity regions were dominated by the microbial food web and the major carbon flow was through the microbial food web to the microzooplankton with a high proportion of the primary production being consumed by the microzooplankton (Azam et al. 1983, 1991, Hall et al. 1999).

ARF (Lutjeharms & Valentine 1984, Belkin & Gordon 1996) is readily distinguishable by its expression in SST that ranged from 20.7 to 17.2°C (mean 18.4°C) and in the subsurface (upper 100 to 150 m) thermohaline fields. The Agulhas Retroflection Current has a core width of ca. 70 km and it transports an estimated 44 ± 5 Sverdrups (Sv = 10^6 m^3 s^{-1}) in the upper 1000 m (Boebel et al. 2003). Between 38° and 40° S it develops a quasi-stationary meandering pattern (wavelength 500 km). The upwelled waters along of the southwest

African coast were advected into the present study area, and this was identified by their relatively high content of nitrate (0.28 μM) (Fig. 5b), chl *a* (0.13 mg m^{-3}) (Fig. 8a) and primary productivity (493 mg C m^{-2} d^{-1}) (Fig. 9). Both chl *a* concentrations and primary production within the Agulhas current system exhibited seasonal patterns (Fig. 8b). SeaWIFS data showed high chl *a* concentrations (0.5 mg m^{-3}) during the austral summer (December) (Fig. 8b). But, instead of a proportionate increase, we observed a drastic decrease (Fig. 11a,b) in the mesozooplankton biomass in this front. On the other hand, microzooplankton was abundant (12.8 × 10^3 ind. m^{-3}) in the surface layer (Fig. 10a). The integrated abundance of microzooplankton in the upper 120 m (Fig. 10b) was 2434 × 10^3 ind. m^{-2} and the community was dominated by ciliates (62%). However, elucidating the food web ecology in such complex situations is very difficult. The mixing of the oligotrophic subtropical water with nutrient-rich Atlantic and Subantarctic waters substantially modifies the system. In such a dynamic system, the current velocities (Boebel et al. 1998) are so high (ca. 200 cm s^{-1}) that they might deter the stabilization of mesozooplankton population and/or the time may not be sufficient for the population to respond to the nutrient enrichment.

Our observation of the mean position of the SSTF front was consistent with that of Lutjeharms & Valentine (1984). SSTF is the bound-
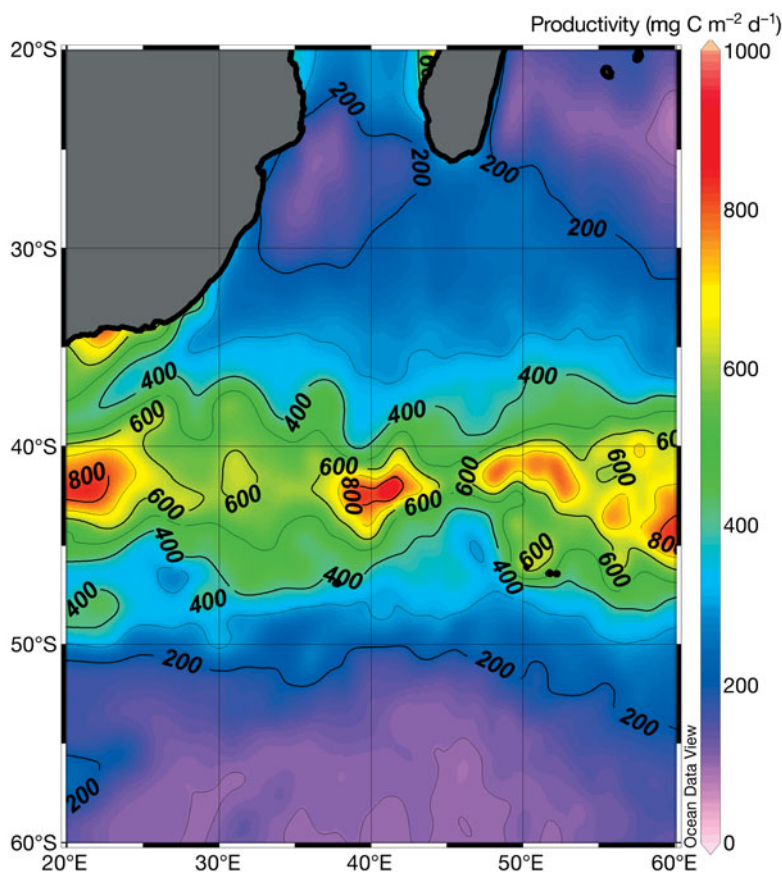

Fig. 9. Water column primary productivity (mg C m^{-2} d^{-1}) computed from remotely sensed data by using vertically generalized production model also showed the high primary production rate at the South Subtropical Front (SSTF)

ary between the warm saline (Fig. 3a,b) subtropical waters and the cool, less saline waters of the Southern Ocean. In the convergence, both chl *a* and column primary production were high (0.47 mg m^{-3} and 950 mg C m^{-2} d^{-1}, respectively) and so also was the mesozooplankton standing stock (1.46 ml m^{-3}). The isopycnal mixing between the subtropical and subantarctic waters introduces nutrient-rich subthermocline waters into the surface layers, thereby augmenting the primary (Fig. 9) and secondary production (Fig. 11a,b). This also enhanced both the surface (14.4 × 10^3 ind. m^{-3}) and column (Fig. 10a,b) (4459 × 10^3 ind. m^{-2}) microzooplankton biomass. Previous studies have recorded that frontal systems are characterised by increased biological productivity and biomass at all trophic levels of the pelagic ecosystem (Lutjeharms et al. 1985, Pakhomov et al. 1994, Pakhomov & McQuaid 1996). The microzooplankton community changes from being totally dominated by ciliates in the subtropical waters to more diverse forms (ciliates 36%, dinoflagellates 38% and nauplii 25%) in the subantarctic waters. This change in microzooplankton population could also be due to a change toward larger phytoplankton favouring populations of larger heterotrophic dinoflagellates rather than ciliates. Hansen (1991) reported the ability of heterotrophic dinoflagellates to graze a wider range of prey, from small cyanobacteria to larger diatoms, as their diverse feeding mechanisms enable them to survive in a variety of environments. During the winter, productivity is probably light-limited, the ciliates dominate in the microzooplankton community and the energy flow is predominantly via the microbial loop. During the spring and summer, since light is not a limiting factor, large phytoplankton blooms occur (Fig. 8b) that can be sustained by the nutrients supplied by the vertical mixing of water. However, high microzooplankton populations are also maintained at the same time implying that the microbial loop is also active during this period.

The SAZ has an almost uniform SST of 8.3°C (Figs. 2 & 3a) and SSS of 33.8 (Fig. 3b) throughout. There is a clear thermostad (Fig. 3a) at 200 to 400 m depth, which forms in the winter as a result of vertical overturn. This is a HNLC zone. To the north, productivity in the subtropical waters is nutrient-limited, whereas to the south, the polar zone is light-limited. Within this region solar irradiance is esti-

mated to be 150 W m^{-2} (day length ca. 9 h) during the winter and rises to 450 W m^{-2} (day length ca. 15 h) during summer. Although the macronutrient supplies in the wind-mixed layer were sufficient to support high productivity, the surface chl *a* (Fig. 8a) concentration (0.18 mg m^{-3}) and column primary productivity (374 mg C m^{-2} d^{-1}) remained low (Fig. 9). Two main hypotheses have been proposed to explain why primary production remains suppressed: (1) grazing pressure reduces the phytoplankton abundance, or (2) lack of essential micronutrients, particularly iron, limits the primary production (Martin et al. 1990a,b). Mesozooplankton standing stocks in this region (Fig. 11a) were similar to those observed in both the subtropical and polar zones (Fig. 11b), but microzooplankton populations showed abundance at the
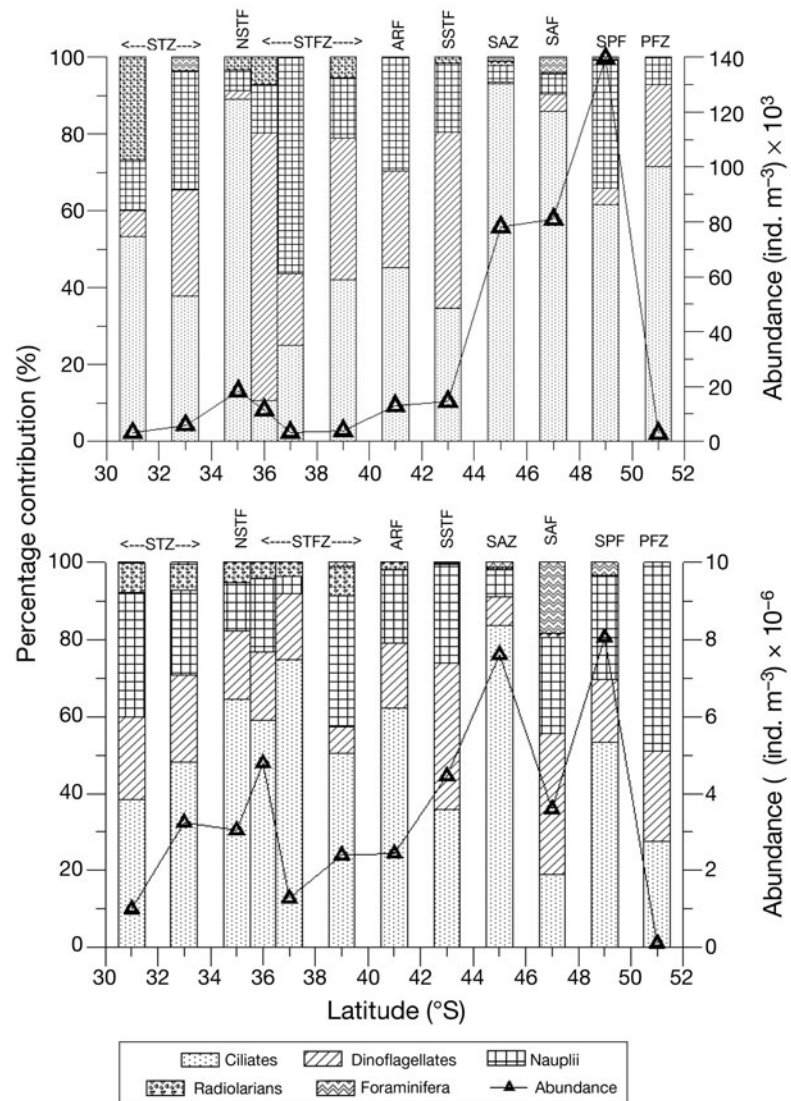

Fig. 10. Variations in the composition of microzooplankton (a) at the surface and (b) in the upper 120 m of the water column of different fronts and zones. See Fig. 3 for abbreviations

surface (79.4×10^3 ind. m^{-3}) and in the upper 120 m column (5608×10^3 ind. m^{-2}) (Fig. 10a,b). This indicates that the primary production in this region is supported by regenerated nutrients and is utilized in the microbial food web. Laubscher et al. (1993) also reported that nanophytoplankton, which support the microzooplankton community, was the dominant component in the interfrontal regions between the SSTF and SAF during late summer.

SST declined from 9.0 to 5.1°C (Lutjeharms & Valentine 1984) across the SAF and SSS declined from 34.11 to 33.89 (Allanson et al. 1981). Belkin & Gordon (1996) defined the front as the boundary between the inter-

mediate salinity minimum and subantarctic mode water (SAMW) thermostad to the north. Despite the high concentrations of nutrients (Fig. 5b–d) (NO$_3$: 21.3, PO$_4$: 0.96 and SiO$_4$: 8.4 µmol), the biological production was low. During winter, low solar irradiance (Fig. 7a,b) and the short day lengths were probably the major limiting factors on productivity. But even during summer, standing stocks of chlorophyll and primary production remained low (Fig. 8a,b) (0.2 mg m^{-2} and 327 mg C m^{-2} d^{-1}, respectively) as did the secondary production for SAF and SST (0.13 and 0.173 ml m^{-3}) (Fig. 11a,b). This finding agrees with earlier studies conducted in the SSAF (Bernard & Froneman 2003).

Microzooplankton abundance both at the surface (80×10^3 ind. m^{-3}) and in the upper 120 m (3600×10^3 ind. m^{-2}) (Fig. 10a,b) was sufficient to support moderate mesozooplankton standing stocks. The composition of the microzooplankton community (Fig. 10b) changed (ciliates 19%, dinoflagellates 36.5% and nauplii 25%). This change in microzooplankton populations could also be due to a change toward larger phytoplankton favouring populations of larger heterotrophic dinoflagellates rather than ciliates. The reduction in ciliate populations was probably related to the development of large diatom blooms, as the diatoms are too large in size for the ciliates to feed on. The other important microzooplankton group, the heterotrophic dinoflagellates, prefer prey of their own size and the linear size ratio between predators and their optimal prey is 1:1; hence, the prey to predator size ratio is crucial for the structuring of pelagic food web (Hansen et al. 1994). Changes in the environmental conditions have been observed to influence the abundance and composition of the microzooplankton community (Atkinson 1996, Hall et al. 1999). A major factor contributing to low biomass of mesozooplankton (Fig. 11a,b) may be the changing environment, i.e. the formation of AAIW and lateral mixing with SAMW, resulting in a sharp drop of 3.0°C in SST. The assemblage of organisms that inhabited the polar region was entirely different from that in the subtropical seas. Even though food resources in the front were potentially high, the sharp shifts in environmental conditions probably inhibited the buildup of standing stocks of zooplankton.

The SPF is a region where SST changes from 6.0 to 2.0°C (mean 3.4°C) and SSS from 33.8 to 33.9. We observed the maximum SST gradient (Figs. 2 & 3a) centered at 3.8°C and SSS at 33.79 (Fig. 3b) is in agreement with
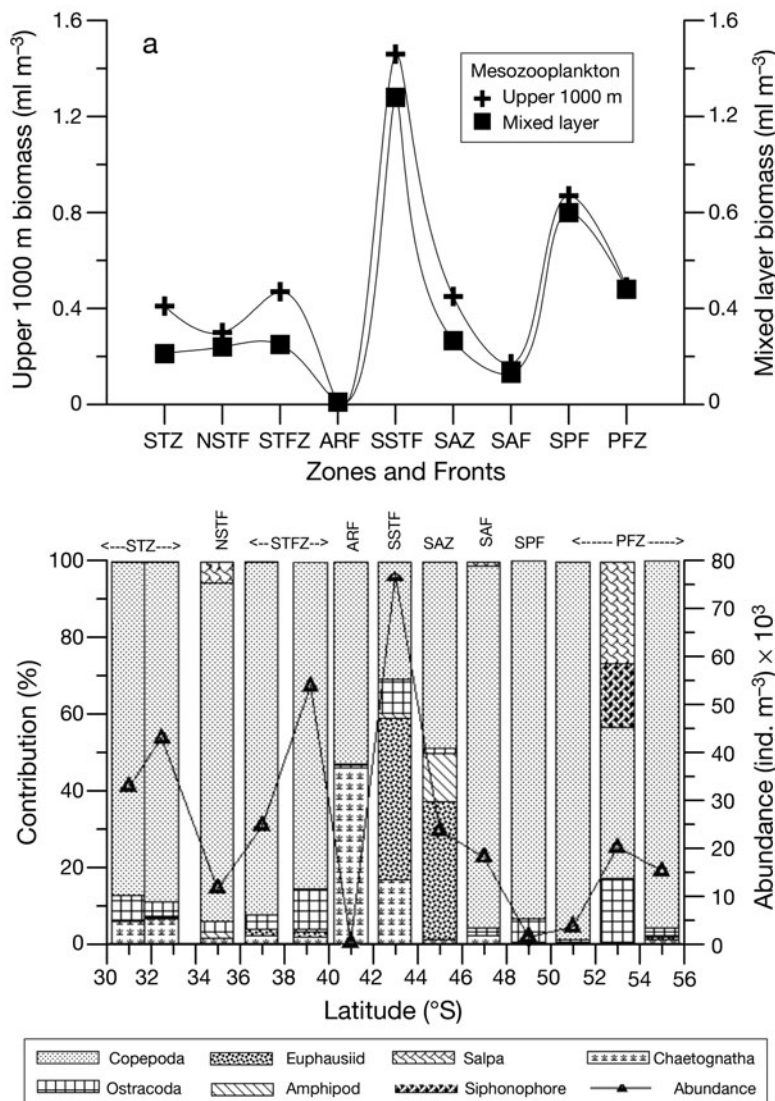

Fig. 11. (a) Variations in the mesozooplankton biomass (ml m^{-3}) in fronts and zones. Uniform biomass can be observed at different zones. (b) Percentage composition of different taxa and total abundances of mesozooplankton (ind. m^{-3}). Copepods were the dominant component in all of the zones and fronts except at the SSF and SAZ. See Fig. 3 for abbreviations

those reported by Allanson et al. (1981). One effect of the ACC (Fig. 4a) is that it caused the isopycnals to outcrop at the surface and, hence, mixing of the high concentration of nutrients occurred from deep water to the surface layers (Sloyan & Rintoul 2001, Pollard et al. 2002). We observed sharp increases in the nutrient concentrations (Fig. 5b–d) (NO_3^-: 26.7, PO_4^-: 0.8 and SiO_4^-: 39.4 µmol) associated with the frontal region. Seasonal fluctuations in solar irradiance and day length (Fig. 7a,b) showed that there was absence of light during the winter, but during summer, despite the sun's low angle of incidence, sufficient light was available for photosynthesis. However, no concomitant general increase in the chl a (Fig. 8a) or water column production (Fig. 9) was observed. It is now recognized that phytoplankton blooms associated with the seasonal ice retreat contribute substantially to the biochemical cycling (Smith & Nelson 1986). However, we observed low chl a (<0.2 mg m^{-3}) and primary production (<200 mg C m^{-2} d^{-1}) (Table 1). Bernard & Froneman (2003) showed that no enhancement of chl a biomass was recorded in the vicinity of PF. Froneman et al. (2000) and Pakhomov & Froneman (2004) found that zooplankton grazing accounted for up to 89% of the daily

primary production in the polar region. Thus, in contrast to the HNLC regions, it appears that high grazing pressure by abundant mesozooplankton standing stock (Fig. 11a,b) and increase of copepod nauplii in the microzooplankton community (Fig. 10a,b) might have limited the buildup of chl a concentrations (phytoplankton bloom). The chl a and primary production levels presented here are substantially lower than those observed in the PF by Allanson et al. (1981) and Lutjeharms et al. (1985). De Baar et al. (1995) correlated high iron concentrations with enhanced primary productivity at PF in the Atlantic sector. Those authors reported that the high primary productivity was supported by the advection of iron-rich water masses within the frontal jet. Ciliates occurred at maximum densities at the surface at 49°S (Fig. 10a), where the surface chl a was 0.18 mg m^{-3}. The contribution of heterotrophic dinoflagellates appears to be higher in the subsurface layers (Fig. 10b), within the pycnocline as well as at the base of the photic zone. These depth profiles may result from the predator/prey interactions, characteristic for microzooplankton consumers, such as ciliates, which generally feed on particles <20 µm in size. During the spring and summer, diatoms can

Table 1. Surface values of physical (temperature [°C]; salinity) and chemical (dissolved oxygen [DO]; nutrients) variables measured across the fronts and zones of the 45°E longitude during austral summer 2004. See Fig. 3 for abbreviations

Zones and fronts	Latitude (°S)	Longitude (°E)	Station depth (m)	Potential temperature (°C)	Salinity	DO (µmol)	NO$_3$ (µmol)	PO$_4$ (µmol)	SiO$_4$ (µmol)
STZ	30.34	45.80	1778	25.31	35.63	221			
	31.01	45.00	2251	25.14	35.66	209	2.66	0.16	6.58
	32.00	45.00	1988	25.00	35.68	215			
	32.84	45.00	1166	23.35	35.69	223	0.66	0.16	5.17
NSTF	34.00	45.00	1100	21.92	35.69	225			
	35.08	45.00	2275	22.22	35.70	225	0.66	0.16	4.39
STFZ	36.14	45.00	2850	21.07	35.68	232			
	36.99	45.00	2979	20.05	35.64	229	0.28	0.16	7.31
	38.01	45.00	3081	20.05	35.62	224			
	39.00	45.00	4004	20.48	35.59	219	0.43	0.16	8.04
ARF	40.43	45.00	3854	18.71	35.60	230			
	41.01	45.00	3256	18.42	35.62	239	0.29	0.10	5.85
SSTF	42.00	45.00	3480	13.06	34.16	286			
SAZ	43.02	45.00	3097	10.23	33.70	307	14.40	0.10	9.50
	44.00	45.00	2205	8.66	33.77	319			
	45.02	45.00	1613	8.43	33.77	307	19.73	0.64	9.50
	46.01	45.00	1897	7.75	33.80	315			
	47.01	45.00	3227	7.24	33.79	317	19.87	0.32	7.31
SAF	47.99	45.00	3927	5.39	33.77	304			
	49.00	45.00	4245	5.23	33.77	335	21.31	0.96	8.04
SPF	49.99	45.00	4383	3.83	33.79	338			
PFZ	51.00	45.00	4051	2.72	33.87	347	26.74	0.80	39.47
	52.00	45.00	3129	2.64	33.88	340			
	53.00	45.00	319	2.35	33.80	350	25.88	0.96	48.97
	54.00	45.00	3876	2.19	33.78	363			
	55.00	45.00	4137	2.24	33.80	326	10.11	0.16	24.12

Table 2. Biological variables measured across the fronts and zones of 45° E longitude during the austral summer 2004. Chl *a*, primary productivity (PP), microzooplankton (micro) abundance in the surface (S) and in the upper 120 m, mesozooplankton (meso) biomass in the mixed layer depth (MLD) and in the upper 1000 m are shown. Biomass values in **bold** letters are those that have similar values in different zones. Anomalous values in brackets. See Fig. 3 for abbreviations

Zones and fronts	Latitude (°S)	Longitude (°E)	Station Depth (m)	Chl *a* (mg m⁻²)	PP (mg C m⁻² d⁻¹)	Micro (S) × 10³ (ind. m⁻³)	Micro (upper 120 m) × 10³ (ind. m⁻³)	Meso (MLD) (ml m⁻³)	Meso (upper 1000 m) (ml m⁻³)
STZ	30.34	45.80	1778	0.085	203.98				
	31.01	45.00	2251	0.091	214.68	4.40	1588	0.21	**0.41**
	32.00	45.00	1988	0.072	205.58				
	32.84	45.00	1166	0.077	233.90				
NSTF	34.00	45.00	1100	0.077	294.99	18.20	3046	0.24	0.30
	35.08	45.00	2275	0.082	295.19				
STFZ	36.14	45.00	2850	0.079	300.86				
	36.99	45.00	2979	0.088	333.99				
	38.01	45.00	3081	0.107	373.23	3.50	2819	0.25	**0.47**
	39.00	45.00	4004	0.125	430.15				
ARF	40.43	45.00	3854	0.123	408.75	12.80	2434	0.01	0.01
	41.01	45.00	3256	0.138	493.02				
SSTF	42.00	45.00	3480	0.479	950.13	14.40	4459	1.28	1.46
SAZ	43.02	45.00	3097	0.195	456.38				
	44.00	45.00	2205	0.159	348.57				
	45.02	45.00	1613	0.170	335.67				
	46.01	45.00	1897	0.188	365.22	79.40	5608	0.27	**0.45**
	47.01	45.00	3227	0.209	367.88				
SAF	47.99	45.00	3927	0.202	338.77	80.80	3600	0.13	0.17
	49.00	45.00	4245	0.224	315.88				
SPF	49.99	45.00	4383	0.125	187.19	139.40	8057	0.80	0.87
PFZ	51.00	45.00	4051	0.091	144.49				
	52.00	45.00	3129	0.062	108.65				
	53.00	45.00	319	0.072	108.01			0.48	**0.50**
	54.00	45.00	3876	0.069	104.34	2.80	108	(6.46)	(6.55)
	55.00	45.00	4137	0.109	119.54				

exploit the eutrophic conditions and develop blooms. We observed the highest microzooplankton (Fig. 10a) abundance both at the surface (140×10^3 ind. m⁻³) and within the upper 120 m (Fig. 10b) (8057×10^3 ind. m⁻²). Here the major constituents of the microzooplankton community were ciliates (53%), nauplii (26.5%) and dinoflagellates (16%). In late summer, both chl *a* (0.125 mg m⁻³) and primary production (187 mg C m⁻² d⁻¹) levels declined. Even then the microzooplankton community (8057×10^3 ind. m⁻²) flourished and sustained high mesozooplankton (Fig. 11a,b) standing stock (0.87 ml m⁻³). Low chl *a* and low primary production rates with high micro- and mesozooplankton biomass establish that both traditional food web and microbial loop pathways were active in this front.

In the PFZ, weak subsurface salinity and temperature minima (Fig. 2) were observed that were concordant with the observation of Allanson et al. (1981). During the spring–summer, ice melt and Antarctic divergent water advected from the Antarctic region stabilised the upper water column, especially where

the isopycnals outcrop because of the ACC (Fig. 4a). This increased water column stability with high nutrient and trace metal concentrations plays a major role in triggering phytoplankton blooms in the vicinity of the polar front (Dubischar & Bathmann 1997, Perissinotto & Pakhomov 1998). Antarctic polar frontal zones are characterised by patches and bands of high chl *a* (Laubscher et al. 1993, Dafner & Mordasov 1994, Bathmann et al. 1997). The growth rates and maximum standing stocks of the large diatom appear to have been regulated by the availability of dissolved silica. Tremblay et al. (2002) reported that along the PF, elevated concentration of chl *a* and primary production and abundance of microzooplankton (>20 to 200 µm) coincided with high dominance of large or long-chained diatoms. Strong nutrient deficits (Figs. 5b–d) were clearly seen in this region. The decrease in the nutrient concentrations (NO_3^-: 10 µM) in this region (Fig. 5b–d) was generally linked with high diatom blooms, but chl *a* concentrations (Fig. 8a) and primary production (Fig. 9) did not correlate with these blooms.

The high grazing pressure of copepods and salps (Fig. 11b), which were abundant at the time of our observations, probably reduced the phytoplankton standing crop and productivity. The stable stratification resulting from the advection of fresher ice-melt water from the ice edge probably prevented vertical mixing of deep water and replenishment of nutrients. These studies highlight the importance of the PF as a biogeographic boundary for zooplankton distribution, demarcating the subantarctic and Antarctic realms of the Southern Ocean. The sharp decrease in the micro-zooplankton abundance in this zone may also be the result of strong grazing pressure by large copepods and carnivorous zooplankton. Copepods were the dominant metazooplankton in the PFZ (Fransz & Gonzalez 1997). The mesozooplankton community was dominated almost entirely by copepods, which agrees with a number of previous studies (Pakhomov & Froneman 1999, Bernard & Froneman 2003, 2005). Within the microzooplankton community, ciliates (25%) were replaced by copepod nauplii (50%), and this probably contributed to the strong grazing pressure. Lugomela et al. (2001) reported that copepod nauplii are an important link between the classical and microbial food webs because of their small size and have the ability to feed on pico-sized particles, which are generally unavailable to the later copepodites and adults. The strong grazing effect of copepods in the PFZ during autumn has been reported (Perissinotto 1992, Bernard & Froneman 2003) and the slightly reduced effect during summer may be attributed to the inability of copepods to consume larger phytoplankton, which dominate total chl *a* (Fortier et al. 1994). The mesozooplankton biomass was 0.5 ml m^{-3}, which was almost equal to that observed in the other zones. Although most of the cyclopoids did not significantly ingest small autotrophic and heterotrophic flagellates (2 to 8 μm), large copepods were actively feeding on particles >10 μm including autotrophic/heterotrophic dinoflagellates and ciliates with a clearance rate of 0.03 to 0.38 ml ind.$^{-1}$ h^{-1} (Nakamura & Turner 1997). Odate (1994) suggested that top-down control of zooplankton might alter the abundance and size composition of phytoplankton in summer, i.e. net zooplankton grazing may suppress the net phyto- and microzooplankton abundance (multivorous food web).

Belkin & Gordon (1996) identified the northern boundary of the subsurface minimum layer, bounded by the 2.0°C isotherm, within the depth range of 100 to 300 m. We observed the SSPF between 51°S and 55°S; the 2.0°C isotherm clearly demarcated the polar waters at both the surface and subsurface layers. Our mean path turns southward at the Ob-lena Rise (46°E). Seamounts and islands are regions of locally enhanced production through the 'island mass effect' (Genin &

Boehlert 1985, Coutis & Middleton 1999), and in HNLC regions by being a source of dissolved iron. The high mesozooplankton abundance (12.8 ml m^{-3}) (Fig. 11a,b, Table 2) observed in this region may be due to the island mass effect. The major contributors of this high biomass were copepods, salps and medusae.

CONCLUSIONS

This study revealed that during the austral summer, mesozooplankton standing stock remained similar in all zones (STZ, STFZ, SAZ and PFZ) of the Indian Ocean sector of the Southern Ocean crossing 45°E meridian, though chl *a* and primary production varied in each zone. The similarity in the mesozooplankton standing stock can be attributed to the functioning of alternate food webs like the microbial loop and the multivorous food web. A chart of solar irradiance and day length showed that light was not a limiting factor for biological productivity in the subtropical region, whereas it was a constraint in the subantarctic and polar regions. While nutrients were the major limiting factor for primary production in the photic zone of the subtropical region, solar irradiance is very low in the SAZ and PFZ. So solar irradiance is the limiting factor for primary production in the SAZ and PFZ. Oligotrophic behaviour of the subtropical region was due to the combined effect of low nutrient concentration in the surface layers and the deep thermocline region that exceeded compensation depth and strong stratifications. Although such a condition existed in this region, the microbial food web played a vital role in maintaining the zooplankton standing stock through high ciliate abundance. Thus, the basic metabolic needs of the mesozooplankton were met by grazing microzooplankton. The dominance of the microzooplankton in the subtropical region is supported by the findings of Bradford-Grieve et al. (1997). In the Agulhas region, availability of sufficient nutrients and primary production made the system eutrophic, but the secondary standing stock was quite low. This may be due to the prevalence of strong currents and a dynamic environment, which would deter the establishment of mesozooplankton communities. Due to the strong circumpolar current and weak stratification maintained by tilting of isopycnals towards the surface in the southern part of ACC, the permanent thermocline reached the surface of SSTF and supplied high amounts of nutrients and CO_2, which could be utilized for biological production. High rates of primary and secondary production suggest the prevalence of an active traditional food web and a high abundance of microzooplankton indicates an active microbial food web is also functioning in this front. The SAZ exhibited

the HNLC phenomenon, but mesozooplankton abundance in this zone was similar to other zones. This was due to the abundance of microzooplankton, which provided the nutritional resources for the mesozooplankton. The PFZ becomes productive during the austral summer by a combined effect of advection of ice melt and Antarctic divergent water together with trace metal concentrations and a stabilised upper water column. However, high grazing pressure exerted by copepods and tunicates decreases the phytoplankton standing stock in the PF and the prevalence of a multivorous food web maintained a secondary standing stock similar to that in other zones. This was supported by replacement of ciliates by copepod nauplii in the microzooplankton community. From the present study it is understood that the similarity in the mesozooplankton standing stock in all the major zones are supported by a microzooplankton community. In the zones, the major share of the primary production could be channelled through the microzooplankton to sustain the mesozooplankton biomass. This illustrates the importance of the microbial food web as a link for the transfer of carbon fixed by small autotrophs to mesozooplankton. Nonetheless, only long-term observations can clearly show whether seasonality has any effect on the mesozooplankton standing stock. Further studies in this direction would provide a better understanding of the intricate relationship underlying the secondary productivity of the Southern Ocean.

LITERATURE CITED

Abrams RW (1985) Energy and food requirements of pelagic aerial seabirds in different regions of the African sector of the Southern Ocean. In: Siegfried WR, Condy PR, Laws RM (eds) Antarctic nutrient cycles and food webs. Springer, Berlin, p 466–472

Allanson BR, Hart RC, Lutjeharms JRE (1981) Observations on the nutrients, chlorophyll and primary production of the Southern Ocean south of Africa. S Afr J Antarct Res 10/11:3–14

Atkinson A (1996) Subantarctic copepods in an oceanic low chlorophyll environment: ciliate predation, low food selec-

tivity and impact on prey populations. Mar Ecol Prog Ser 130:85–96

Azam F, Smith DC, Hollibaugh JT (1991) The role of the microbial loop in Antarctic pelagic ecosystems. Polar Res 10:239–243

Azam F, Fenchel T, Field JG, Gray JS, Meyer-Reil LA, Thingstad F (1983) The ecological role of water-column microbes in the sea. Mar Ecol Prog Ser 10:257–263

Bathmann UV, Scharek R, Klaas C, Dubischar CD, Smetacek V (1997) Spring development of phytoplankton biomass and composition in major water masses of the Atlantic sector of the Southern Ocean. Deep-Sea Res II 44:51–67

Behrenfield MJ, Falkowski PG (1997a) A consumer's guide to phytoplankton primary productivity models. Limnol Oceanogr 42:1479–1491

Behrenfield MJ, Falkowski PG (1997b) Photosynthetic rates derived from satellite-based chlorophyll concentration. Limnol Oceanogr 42:1–20

Belkin IM, Gordon AL (1996) Southern Ocean fronts from the Greenwich Meridian to Tasmania. J Geophys Res 101: 3675–3696

Bernard KS, Froneman PW (2003) Mesozooplankton community structure and grazing impact in the Polar Frontal Zone of the south Indian Ocean during austral autumn 2002. Polar Biol 26:268–275

Bernard KS, Froneman PW (2005) Trophodynamics of selected mesozooplankton in the west-Indian sector of the Polar Frontal Zone, Southern Ocean. Polar Biol 28: 594–606

Boebel O, Rae CD, Garzoli S, Lutjeharms J, Richardson P, Rossby T, Schmid C, Zenk W (1998) Float experiment studies interocean exchanges at the tip of Africa. EOS Trans Am Geophys Union 79(1):1

Boebel O, Rossby T, Lutjeharms J, Zenk W, Barron C (2003) Path and variability of the Agulhas Return Current. Deep-Sea Res II 50:35–56

Boyd PW, Watson AJ, Law CS, Abraham ER and others (2000) A mesoscale phytoplankton bloom in the polar Southern Ocean stimulated by iron fertilization. Nature 407: 695–730

Bradford-Grieve JM, Chang FH, Gall M, Pickmere S, Richards F (1997) Size fractionated phytoplankton standing stocks and primary production during Austral winter and spring 1993 in the subtropical convergence near New Zealand. N Z J Mar Freshw Res 31:201–224

Calbet A, Landry MR, Nunnery S (2001) Bacteria flagellate interactions in the microbial food web of the oligotrophic subtropical North Pacific. Aquat Microb Ecol 23:283–292

Carpenter JH (1965) The Chesapeake Bay Institute technique for the Winkler dissolved oxygen method. Limnol Oceanogr 10:141–143

Coutis PF, Middleton JH (1999) Flow topography interaction in the vicinity of an isolated deep ocean island. Deep-Sea Res II 46:1633–1652

Dafner EV, Mordasov NV (1994) Influence of biotic factors on the hydrochemical structure of surface water in the Polar Frontal Zone of the Atlantic Antarctic. Mar Chem 45: 137–148

De Baar HJW, de Jong JTM, Baker DCE (1995) Importance of iron for plankton blooms and carbon dioxide draw down in the Southern Ocean. Nature 373:412–415

Deacon GER (1933) A general account of the hydrology of the South Atlantic Ocean. Discov Rep 7:171–238

Deacon GER (1937) The hydrology of the Southern Ocean. Discov Rep 15:122–123

Deacon GER (1982) Physical and biological zonation in the Southern Ocean. Deep-Sea Res II 29:1–16

Deacon GER (1983) Kerguelen, Antarctic and subantarctic. Deep-Sea Res I 30:77–81

Detmer A, Bathmann U (1997) Distribution patterns of autotrophic pico- and nanoplankton and their relative contribution to algal biomass during spring in the Atlantic sector of the Southern Ocean. Deep-Sea Res II 44:299–320

Dubischar CD, Bathmann UV (1997) Grazing impact of copepods and salps on phytoplankton in the Atlantic sector of the Southern Ocean. Deep-Sea Res II 44:415–433

El-Sayed S (1984) Productivity of the Antarctic waters — a reappraisal. In: Holm-Hansen O, Bolis L, Gilles R (eds) Marine phytoplankton and productivity. Springer, Berlin, p 19–34

Fielding S, Ward P, Pollard RT, Seeyave S, Read JF, Hughes JA, Smith T, Castellani C (2007) Community structure and grazing impact of mesozooplankton during late spring/ early summer 2004/2005 in the vicinity of the Crozet Islands (Southern Ocean). Deep-Sea Res II 54: 2106–2125

Fortier L, Le Fevre J, Legendre L (1994) Export of biogenic carbon to fish and to the deep ocean: the role of large planktonic microphages. J Plankton Res 16:809–839

Fransz HG, Gonzalez SR (1997) Latitudinal metazoan plankton zones in the antarctic circumpolar current along 6°W during austral spring 1992. Deep-Sea Res II 44:395–414

Froneman PW, Pakhomov EA, Perissinotto R, McQuaid CD (2000) Zooplankton structure and grazing in the Atlantic sector of the Southern Ocean in late austral summer 1993: Part 2. Biochemical zonation. Deep-Sea Res I 47: 1687–1702

Froneman PW, Ansorge IJ, Richoux N, Blake J and others (2007) Physical and biological processes at the subtropical convergence in the south-west Indian ocean. S Afr J Sci 103:193–195

Genin A, Boehlert GW (1985) Dynamics of temperature and chlorophyll structures above a seamount: an oceanic experiment. J Mar Res 43:907–924

Gordon AL (1985) Indian–Atlantic transfer of thermocline water at the Agulhas retroflection. Science 227:1030–1033

Grachev DG (1991) Frontal zone influences on the distribution of different zooplankton groups in the central part of the Indian sector of the Southern Ocean. In: Samolova MS, Shumkova SO (eds) Ecology of commercial marine hydrobionts. TINRO Press, Vladivostok, p 19–21

Grasshoff K, Ehrhardt M, Kremling K (eds) (1983) Methods of seawater analysis, 2nd edn. Verlag Chemie, Weinheim

Hall JA, James MR, Bradford-Grieve JM (1999) Structure and dynamics of the pelagic microbial food web of the Subtropical Convergence region east of New Zealand. Aquat Microb Ecol 20:95–105

Hansen PJ (1991) Quantitative importance and trophic role of HDS in a coastal pelagic food web. Mar Ecol Prog Ser 73: 253–273

Hansen B, Bjornsen PK, Hansen PJ (1994) The size ratio between planktonic predators and their prey. Limnol Oceanogr 39:395–403

Holliday NP, Read JF (1998) Surface oceanic fronts between Africa and Antarctica. Deep-Sea Res I 45:217–238

Huntley ME, Lopez MDG, Karl DM (1991) Top predators in the Southern Ocean: a major leak in the biological carbon pump. Science 253:64–66

Jaspers C, Nielsen TG, Carstensen J, Hopcroft RR, Moller EF (2009) Metazooplankton distribution across the Southern Indian Ocean with emphasis on the role of Larvaceans. J Plankton Res 31:525–540

Jones EP, Nelson DM, Treguer P (1990) Chemical oceanography. In: Smith WO Jr (ed) Polar oceanography, part B: chemistry, biology and geology, Academic Press, San Diego, CA, p 407–476

Karstensen J, Quadfasel D (2002) Water subducted into the Indian Ocean subtropical gyre. Deep-Sea Res 49: 1441–1457

Kostianoy AG, Ginzburg AI, Lebedav SA, Frankignoulle M, Delille B (2003) Fronts and mesoscale variability in the Southern Indian Ocean as inferred from the TOPEX/ POSEIDON and ERS-2 altimetry data. Oceanology 43: 632–642

Kostianoy AG, Ginzburg AI, Frankignoulle M, Delille B (2004) Fronts in the Southern Indian Ocean as inferred from satellite sea surface temperature data. J Mar Syst 45:55–73

Laubscher RK, Perissinotto R, McQuaid CD (1993) Phytoplankton production and biomass at frontal zones in the Atlantic sector of the Southern Ocean. Polar Biol 13: 471–481

Lugomela C, Wallberg P, Nielsen TG (2001) Plankton composition and cycling of carbon during the rainy season in a tropical coastal ecosystem, Zanzibar, Tanzania. J Plankton Res 23:1121–1136

Lutjeharms JRE (1981) Spatial scales and intensities of circulation in the ocean areas adjacent to South Africa. Deep-Sea Res II 28:1289–1302

Lutjeharms JRE, Valentine HR (1984) Southern Ocean thermal fronts south of Africa. Deep-Sea Res I 31:1461–1475

Lutjeharms JRE, Walters NM, Allanson BR (1985) Oceanic frontal systems and biological enhancement. In: Siegfried WR (ed) Antarctic nutrient cycles and food webs. Springer, Berlin, p 11–21

Lutjeharms JRE, Valentine HR, van Ballegooyen RC (1993) The Subtropical Convergence in the South Atlantic Ocean. S Afr J Sci 89:552–559

Martin JH, Fitzwater SE, Gordon RM (1990a) Iron deficiency limits plankton growth in Antarctic waters. Global Biogeochem Cycles 4:5–12

Martin JH, Gordon RM, Fitzwater SE (1990b) Iron in Antarctic waters. Nature 345:156–158

Morel A, Berthon J (1989) Surface pigments, algal biomass profiles, and potential production of the euphotic layer: relationships reinvestigated in view of remote-sensing applications. Limnol Oceanogr 34:1545–1562

Nakamura Y, Turner JT (1997) Predation and respiration by the small cyclopoid copepod *Oithona similis*: How important is feeding on ciliates and heterotrophic flagellates? J Plankton Res 19:1275–1288

Nelson DM, Smith WO Jr (1991) Sverdrup re-visited: critical depths, maximum chlorophyll levels, and the control of Southern Ocean productivity by the irradiance-mixing regime. Limnol Oceanogr 36:1650–1661

Nielsen TG, Bjornsen PK, Boonruang P, Fryd M and others (2004) Hydrography, bacteria and protist communities across the continental shelf and shelf slope of the Andaman Sea (NE Indian Ocean). Mar Ecol Prog Ser 274:69–86

Odate T (1994) Plankton abundance and size structure in the northern North Pacific Ocean, early summer. Fish Oceanogr 3:267–278

Pakhomov EA, Froneman PW (1999) Macroplankton/ micronekton dynamics in the vicinity of the Prince Edward Islands (Southern Ocean). Mar Biol 134:501–515

Pakhomov EA, Froneman PW (2004) Zooplankton dynamics in the eastern Atlantic sector of the Southern Ocean during the austral summer 1997/1998, Part 2. Grazing impact. Deep-Sea Res II 51: 1663–1686

Pakhomov EA, McQuaid CD (1996) Distribution of surface zooplankton and seabirds across the Southern Ocean. Polar Biol 16:271–286

Pakhomov EA, Perissinotto R, McQuaid CD (1994) Compara-
tive structure of the macrozooplankton/micronekton com-
munities of the Subtropical and Antarctic Polar Fronts.
Mar Ecol Prog Ser 111:155–169

Perissinotto R (1992) Mesozooplankton size-selectivity and
grazing impact on the phytoplankton community of the
Prince Edward Archipelago (Southern Ocean). Mar Ecol
Prog Ser 79:243–258

Perissinotto R, Pakhomov EA (1998) The trophic role of the
tunicate *Salpa thompsoni* in the Antarctic marine ecosys-
tem. J Mar Syst 17:361–374

Pollard RT, Read JF (2001) Circulation pathways and trans-
port of the Southern Ocean in the vicinity of the Southwest
Indian Ridge. J Geophys Res 106:2881–2898

Pollard RT, Bathmann U, Dubischar C, Read JF, Lucas M
(2002) Zooplankton distribution and behaviour in the
Southern Ocean from surveys with a towed optical plank-
ton counter. Deep-Sea Res II 42:641–673

Sakshaug E, Slagstad D, Holm-Hansen O (1991) Factors con-
trolling the development of phytoplankton blooms in the
Antarctic Ocean—a mathematical model. Mar Chem 35:
259–271

Satapoomin S, Nielsen TG, Hansen PJ (2004) Andaman Sea
copepods: spatio-temporal variations in biomass and pro-
duction, and role in the pelagic food web. Mar Ecol Prog

Ser 274:99–122

Sathyendranath S, Platt T (1988) The spectral irradiance field
at the surface and in the interior of the ocean: a model for
applications in oceanography and remote sensing. J Geo-
phys Res 93:9270–9280

Sloyan BM, Rintoul SR (2001) Circulation, renewal and modi-
fication of Antarctic mode and intermediate water. J Phys
Oceanogr 31:1005–1030

Smith WO Jr, Nelson DM (1986) Importance of ice edge
phytoplankton production in the Southern Ocean. Bio-
Science 36:251–257

Strickland JDH, Parsons TR (1972) A practical handbook of
seawater analysis. Bull Fish Res Board Can 167, Ottawa

Taguchi SH, Saito H, Kasai T, Kono T, Kawasaki Y (1992)
Hydrography and spatial variability in the size distribution
of phytoplankton along the Kurilie Islands in the western
subarctic Pacific Ocean. Fish Oceanogr 1:227–237

Tremblay JE, Lucas MJ, Kattner G, Pollard R, Strass VH,
Bathmann UV (2002) Significance of the Polar Frontal
Zone for large-sized diatoms and new production during
summer in the Atlantic sector of the Southern Ocean.
Deep-Sea Res II 49:3793–3811

UNESCO (1994) Protocols for the joint global ocean flux study
(JGOFS) core measurements. Scientific Committee on
Oceanic Research, IOC Manual and Guides No. 29, Paris